Journal of Physics: Conference Series

3D Etching profile evolution simulations: Time dependence analysis of the profile charging during SiO_2 etching in plasma

To cite this article: Branislav Radjenovi and Marija Radmilovi-Radjenovi 2007 *J. Phys.: Conf. Ser.* **86** 012017

View the article online for updates and enhancements.

Related content

- Effects of Mask Pattern Geometry on Plasma Etching Profiles
Hiroshi Fukumoto, Koji Eriguchi and Kouichi Ono
- Role of CF_2 in the etching of SiO_2, Si_3N_4 and Si in fluorocarbon plasma
Chen Lele, Zhu Liang, Xu Linda et al.
- Si and SiO_2 Etching under Low Self-Bias Voltage
Tsunetoshi Arikado and Yasuhiro Horiike

Recent citations

- The interplay between surface charging and microscale roughness during plasma etching of polymeric substrates
George Memos *et al*
- Dust Plasma Effect on the Etching Process of Si[100] by Ultra Low Frequency RF Plasma
Ahmed Rida Galaly and Farouk Fahmi Elakshar
- Top down nano technologies in surface modification of materials
Branislav Radjenović and and Marija Radmilovi-Radjenovi

This content was downloaded from IP address 147.91.4.60 on 07/03/2018 at 13:55

3D Etching profile evolution simulations: Time dependence analysis of the profile charging during SiO_2 etching in plasma

Branislav Radjenović[1] and Marija Radmilović-Radjenović[2]

[1] Laboratory of Physics, Vinča Institute of Nuclear Sciencies,

P.O. Box 522, 11001 Belgrade, Serbia

[2] Institute of Physics, Pregrevica 118, 11080 Belgrade, Serbia

E-mail: bradjeno@vin.bg.ac.yu

Abstract. The ability to simulate feature charging was added to the 3D level set profile evolution simulator described earlier. A comprehensive simulation of etching profile evolution requires knowledge of the etching rates at all the points of the profile surface during the etching process. Electrons do not contribute directly to the material removal, but they are the source, together with positive ions, of the profile charging that has many negative consequences on the final outcome of the process especially in the case of insulating material etching. The ion and electron fluxes were computed along the feature using Monte Carlo method. The surface potential profiles and electric field for the entire feature were generated by solving Laplace equation using finite elements method. Calculations were performed in the case of simplified model of Ar^+/CF_4 non-equilibrium plasma etching of SiO_2. The time dependence of the profile charging during SiO_2 etching in plasma is presented.

1. Introduction

Refined control of etched profile in microelectronic devices during plasma etching process is one of the most important tasks of front-end and back-end microelectronic devices manufacturing technologies. The profile surface evolution itself in plasma etching, deposition and lithography development is a significant challenge for numerical methods for interface tracking itself. Level set methods for evolving interfaces [1, 2] are specially designed for profiles which can develop sharp corners, change topology and undergo orders of magnitude changes in speed. A number of 2D profile simulators are developed that enables modeling of etching profile evolution for many different plasma processing conditions. They are mostly adequate for analyzing long trenches which have inherently a 2D character, or for 3D feature having advantageous symmetry, such as circular vias. However the comparison [3] of otherwise identical 2D infinite trench and 3D finite length trenches shows that 2D models underpredict etch rate and required over-etch to clear trench corners and that proximity to 3-plane corners produces significant side-wall curvature. Besides, as feature dimensions shrink , a thorough understanding of the fundamental mechanisms and the effects occurring at three-dimensional topologies, like as corners etc, which determine etching anisotropy is required to facilitate better

© 2007 IOP Publishing Ltd

process modeling. Predictive 3D profile simulation has been long sought as a means to reduce the time and cost associated with trial-and-error process development and/or etching equipment design.

Additionally, etching submicron features in insulating material such as SiO_2 or materials masked with insulators, e.g., photoresist-masked polysilicon, is accompanied by feature charging effects caused by the differences in electron and ion angular distributions. Plasma charging was first reported by Yoshida in 1983 [4]. Hashimoto described its origin as a consequence of the electron shading mechanism [5]. This effect induces many serious plasma process induced damage problems such as bowing, trenching, reactive ion etching lag, and notching [6]. The reduction in the device size and multilayer structures requires a high-aspect ratio in the SiO_2 etching. As the aspect ratio increases, the charging effect becomes more profound. Damage to integrated circuits during manufacturing as a result of charging of the dielectrics during finalization of interconnects is both reducing the profitability and reducing the ability to reach large sizes of microchips and make complex system integration on a single chip. So, realistic three dimensional etching profile simulations that include charging effects are urgently needed, but still lacking.

In this paper we present some new results of our efforts to include charging effects in 3D level set etching profile simulator developed earlier. We describe shortly the most important ingredients of the etching profile simulation procedure: the profile surface movement via level set method, particle fluxes calculations using Monte-Carlo method and the electric field (generated by the profile charge) calculations on the basis of the finite elements method. Some problems arising in the integration of these major simulation components are discussed. Also, an analysis of the time dependence of the profile charging during SiO_2 etching in plasma for various feature aspect ratios is presented. Although a complete self-consistent cycle that includes profile charging and its influence on the charged particles motion is already implemented, we do not have representative results yet. So, here we present some results of the profile charging calculations for the fixed profile surfaces.

2. Level set method

The basic idea behind the level set method is to represent the surface in question at a certain time t as the zero level set (with respect to the space variables) of a certain function $\varphi(t, \mathbf{x})$, the so called level set function. The initial surface is given by $\{\mathbf{x} \mid \varphi(0, \mathbf{x}) = 0\}$. The evolution of the surface in time is caused by “forces” or fluxes of particles reaching the surface in the case of the etching process. The velocity of the point on the surface normal to the surface will be denoted by $V(t, \mathbf{x})$, and is called velocity function. For the points on the surface this function is determined by physical models of the ongoing processes; in the case of etching by the fluxes of incident particles and subsequent surface reactions. The velocity function generally depends on the time and space variables and we assume that it is defined on the whole simulation domain. At a later time $t > 0$, the surface is as well the zero level set of the function $\varphi(t, \mathbf{x})$, namely it can be defined as a set of points $\{\mathbf{x}\in\Re^n \mid \varphi(t, \mathbf{x}) = 0\}$. This leads to the level set equation

$$\frac{\partial \varphi}{\partial t} + V(t,\mathbf{x})\left|\nabla \varphi\right| = 0, \tag{1}$$

in the unknown function $\varphi(t, \mathbf{x})$, where $\varphi(0, \mathbf{x}) = 0$ determines the initial surface. Having solved this equation the zero level set of the solution is the sought surface at all later times. Actually, this equation relates the time change to the gradient via the velocity function. In the numerical implementation the level set function is represented by its values on grid nodes, and the current surface must be extracted from this grid. In order to apply the level set method a suitable initial function $\varphi(0, \mathbf{x})$ has to be defined first. The natural choice for the initialization is the signed distance function of a point from the given surface. This function is the common distance function multiplied by -1 or +1 depending on which side of the surface the point lies on. As already stated, the values of the velocity function are determined by the physical models. In the actual numerical implementation spatial derivatives of φ are represented using the Engquist-Osher upwind finite difference scheme, or by ENO (higher-order essentially non-oscillatory) and WENO (weighted essentially non-oscillatory) discretizations, that

requires the values of this function at the all grid points considered. The resulting semi-discrete equations can be solved using explicit Euler method, or more precisely by TVD (total-variation diminishing) Runge-Kutta time integration (see ref. [1, 2] for the details).

Several approaches for solving level set equations exist which increase accuracy while decreasing computational effort. They are all based on using some sort of adaptive schemes. The most important are narrow band level set method [1], widely used in etching process modeling tools, and recently developed sparse-filed method [7], implemented in medical image processing ITK library [8]. The sparse-field method use an approximation to the distance function that makes it feasible to recompute the neighborhood of the zero level set at each time step. In that way, it takes the narrow band strategy to the extreme. It computes updates on a band of grid points that is only one point wide. The width of the neighborhood is such that derivatives for the next time step can be calculated. This approach has several advantages. The algorithm does precisely the number of calculation needed to compute the next position of the zero level set surface. The number of points being computed is so small that it is feasible to use a linked-list to keep a track of them, so at each iteration only those points are visited whose values control the position of the zero level set surface. As a result, the number of computations increases with the size of the surface, rather than with the resolution of the grid. In fact, the algorithm is analogous to a locomotive engine that lays down tracks before it and picks up them up behind.

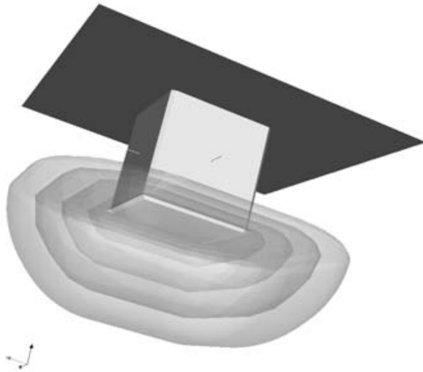

Fig. 1. Isotropic etching - etching profiles at t =0, t = 5 s, t = 10 s, t = 15 s and t = 20 s.

Fig. 2. Optimized Lax-Friedrichs scheme - etching profiles for $V = V_0 \cos\theta$ at t = 0, t = 30s, t = 60s, t = 90s and t = 120s.

Here we will present some calculations illustrating our approach for etching profile evolution simulation. All the calculations are performed on 128×128×384 rectangular grid. The initial profile surface is a rectangle deep with dimensions $0.1 \times 0.1 \times 0.1$ μm. Above the profile surface is the trench region. From its top the particles involved in etching process come from, while bellow is the non-etched material. The actual shape of the initial surface can be described using simple geometrical abstractions. In the beginning of the calculations this description is transformed to the initial level set function using fast marching method [1]. The evolution of the etching profile surface with time is shown in the following figures. In Fig. 1 the results obtained for a test calculation performed with constant velocity function $V = V_0 = 5$ *nm/s* (purely isotropic etching case) are shown. It is supposed that only the bottom surface could be etched; i.e. that the top and the vertical surfaces belong to photo-resist layer. Behavior of the etching profile is as expected.

The equation (1) can be rewritten in Hamilton–Jacobi form

$$\frac{\partial \varphi}{\partial t} + H(\nabla \varphi(t,x)) = 0, \quad (1)$$

where Hamiltonian is given by $H = V(t, \mathbf{x})|\nabla\varphi(t, \mathbf{x})|$ (in this context the term "Hamiltonian" denotes a Hamiltonian function, not an operator). A detailed exposition about the Hamilton–Jacobi equation, the existence and uniqueness of its solution (especially about its viscosity solutions), can be found in [9]. We say that such a Hamiltonian is convex (in $\Re^n$) if the following condition is fulfilled

$$\frac{\partial^2 H}{\partial \varphi_{x_i} \partial \varphi_{x_j}} \geq 0, \quad (2)$$

where φ_{x_i} is a partial derivative of $\varphi(t,\mathbf{x})$ with respect of x_i . If the surface velocity $V(t,\mathbf{x})$ does not depend on the level set function $\varphi(t,\mathbf{x})$ itself, this condition is usually satisfied. In that case, we can say that the problem is of free boundary type.

The non-convex Hamiltonians are characteristic for plasma etching and deposition simulations. During these processes the etching (deposition) rate, that defines the surface velocity function $V(t,\mathbf{x})$, depends on the geometric characteristics of the profile surface itself, or more precisely, on the angle of the incidence of the incoming particles. In the cases under study here we shall consider an etching beam coming down in the vertical direction. These conditions are characteristic for ion milling technology, but angular dependence of the etching rates appears, more or less, in all etching processes.

The upwind (ENO, WENO) difference scheme cannot be used in the case of non-convex Hamiltonians. The simplest scheme that can be applied in these cases is the Lax–Friedrichs, one which relies on the central difference approximation to the numerical flux function, and preserves monotonicity through a second-order linear smoothing term [1, 2]. In [10] we have shown show that it is possible to use the Lax–Friedrichs scheme in conjunction with the sparse field method, and to preserve sharp interfaces and corners by optimizing the amount of smoothing in it. This is of special importance in the simulations of the etching processes in which spatially localized effects appear, like notching and microtrenching.

In the case of the ion enhanced chemical etching the dependence of the surface velocity on the incident angle is simple [11]: $V = V_0 \cos\theta$. The pure chemical etching velocity, or more precisely the etching yield, does not depend on the incident angles. This case can be safely treated by the upwind scheme and using the Lax–Friedrichs scheme would lead to unnecessary rounding of the profile surface. The high aspect ratio (depth/width) etching is a common situation in semiconductor technologies. In the Fig. 2 the evolution of the etching profile, when etching rate is proportional to $V = V_0 \cos\theta$, is presented. This is the simplest form of angular dependence, but it describes the ion enhanced chemical etching process correctly. In this case we expect that the horizontal surfaces move downward, while the vertical ones stay still. This figure shows that it with optimal amount of smoothing gives minimal rounding of sharp corners, while preserving the numerical stability of the calculations. Actually, this is one of the most delicate problems in the etching profile simulations.

3. Calculations of the particle fluxes

A comprehensive simulation of etching requires knowledge of the etching rates at all the points of the profile surface during the etching process. These rates are directly related to fluxes of the etching species on the profile surface, which are themselves determined by the plasma parameters in the etching device. Electrons do not contribute directly to the material removal, but they are the source, together with positive ions, of the profile charging that has many negative consequences on the final outcome of the process especially in the case of insulating material etching, SiO_2 for example. The energy and angular distribution functions for Ar^+ ions (IEDF, IADF) and electrons (EEDF, EADF) are shown in Fig. 3. They are obtained by particle-in-cell (PIC) calculations using XPDC1 code [12, 13]. These data are used as the boundary conditions for the calculations of ion fluxes incident on the profile surface. Collisions in the simulation domain are neglected because mean-free path of ions and

electrons is much longer than the simulation domain size. Also, the probability that more than two particles exist in the simulation space at the same time is very low because the life time of ions or electrons in the simulation region is much shorter than the incident time interval.

Our simulation concept [14] is similar in spirit to the 2D simulations presented in [15-19] and especially [20], where charging effects in 3D rectangular trench were analyzed. Monte Carlo

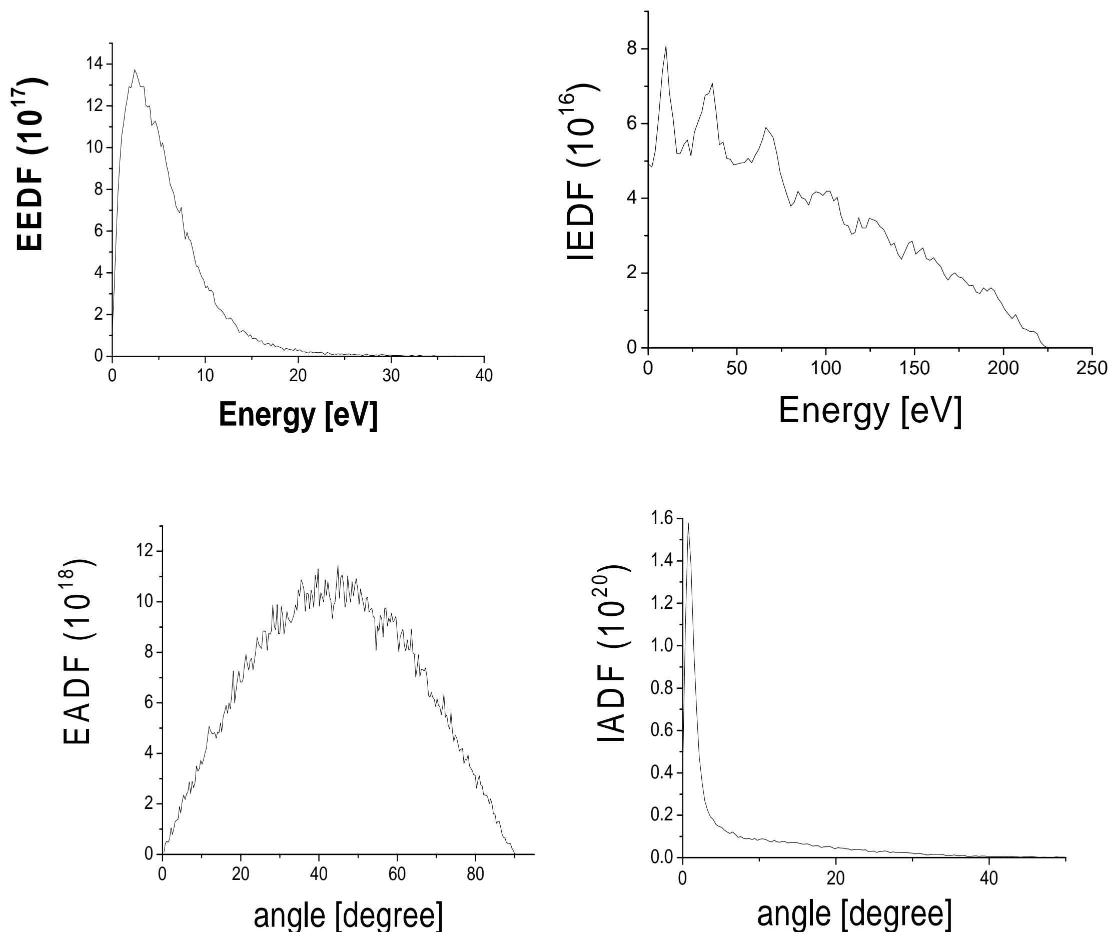

Fig 3. The energy and angular distribution functions for Ar^+ ions (IEDF, IADF) and electrons (EEDF, EADF)

technique is the only feasible method for calculating particle fluxes in 3D geometries. Trench wall charging strongly influences the charged particles motion and, consequently, particle fluxes which themselves determine the local etching rates. Since the trench boundaries have no regular (rectangular) shape in our simulation, finite element calculations was used for the calculation of the electric field. As the etching profile is not known in advance (it is a result of the calculations itself), the problem of meshing is extremely difficult.

The etching process in medium/high density fluorocarbon plasmas is believed to consist of concurrent etching (of the SiO_2 substrate in our case) and deposition (of a fluorocarbon polymer layer) phenomena [11], [21, 22]. Here the deposition process is neglected for the sake of simplicity. So, we consider only a simple case of chemical etching of SiO_2 under Ar^+ ions bombardment. It is also assumed that the electrons are absorbed at the hitting points, while the neutrals can be absorbed or diffusively reflected, once or many times depending on its sticking coefficient. The positive ions can be absorbed, or specularly reflected, depending on their energy and incident angle. It is assumed that

charged particles pass on their charge when they hit the surface, and that this charge does not move after that, what is reasonable for insulating materials. At the boundaries above the profile surface, periodic conditions are assumed.

The surface neutrals coverage (i.e. the fraction of surface covered by free radicals) θ_n statisfy the following balance equation:

$$\frac{d\theta_n}{dt} = J_n S_n (1-\theta_n) - k_{ni} J_{ion} Y_{ni}^{eff} \theta_n - k_{ev} J_{ev} \theta_n , \tag{3}$$

where J_n and J_{ion} are neutral and ion fluxes, S_n is neutral sticking coefficient, k_{ni} and k_{ev} are etchant stoichiometry factors, and Y_{ni}^{eff} is effective etching yield for ion-enhanced chemical etching. Here by the term 'effective' we denote a quantity related to the integral flux, not to an individual particle. J_{ev} is evaporation flux that corresponds to pure chemical etching. It is related to the neutrals flux by Arrhenius law:

$$J_{ev} = K_{SiO_2} e^{-\frac{E_{SiO_2}}{k_b T}} J_n , \tag{4}$$

Balance condition $d\theta_n / dt = 0$ gives the equilibrium surface coverage:

$$\theta_n = \frac{J_n S_n}{J_n S_n \theta_n + k_{ni} J_{ion} Y_{ni}^{eff} + k_{ev} J_{ev}} . \tag{5}$$

So, now we can write equation defining the etching rate ER in the form

$$ER = \frac{1}{\rho_{SiO_2}} [J_{ion} Y_{ni}^{eff} \theta_n + J_{ion} Y_{sp}^{eff} (1-\theta_n) + J_{ev} \theta_n] , \tag{6}$$

where ρ_{SiO_2} is SiO_2 density and Y_{sp}^{eff} is the effective physical spattering etching yield. The etching rate ER defines the velocity function $V(t,\mathbf{x})$ at the profile surface. In actual calculation the feature profile surface is represented by a set of connected triangles, and the above formula should be applied to the every single particular triangle. So, instead of effective etching yields we should define etching yields for every particular ion:

$$Y_{ni}(E_i, \alpha_i) = A_{ni} (\sqrt{E_i} - \sqrt{E_{in}^{th}}) \cos \alpha_i , \tag{7}$$

and

$$Y_{sp}(E_i, \alpha_i) = A_{sp} (\sqrt{E_i} - \sqrt{E_{sp}^{th}}) \cos \alpha_i (1 + B_{sp} \sin^2 \alpha_i) , \tag{8}$$

where E_i is the ion energy and α_i is the angle between the surface normal and the ion incident direction at the point of incidence. Numerical values of the constants appearing in relations (3), (4), (6), (7) and (8) are taken from the reference [19]. The triangular representation of the profile surface requires that instead of integral particle fluxes J_n and J_{ion}, corresponding summations over every particle incident on the particular triangle

$$J_n = \frac{R_n}{A \Delta t_{etch}} N_n , \tag{9}$$

$$J_{ion} Y_{ni}^{eff} = \frac{R_{ion}}{A \Delta t_{etch}} \sum_i Y_{ni}(E_i, \alpha_i) , \tag{10}$$

and

$$J_{ion} Y_{sp}^{eff} = \frac{R_{ion}}{A \Delta t_{etch}} \sum_i Y_{sp}(E_i, \alpha_i) , \tag{11}$$

should be used. Here N_n denotes the number of neutrals absorbed on the particular triangle, R_n (R_{ion}) is the ratio of actual number of neutrals (ions) passing the upper computational domain boundary during the etching time interval and number of neutrals (ions) used in Monte Carlo calculations, A is the particular triangle area, and Δt_{etch} is etching time interval. The ions can be absorbed, or specularly reflected, depending on their energy and incident angle. The probability of specular reflection P_d is given by [23]:

$$P_d = 1 - C_1 \sqrt{E_i} (\frac{\pi}{2} - \alpha_i) . \tag{12}$$

In Fig. 4 some preliminary results of the simulation of a highly anisotropic case, that includes both pure and ion-enhanced chemical etching mechanisms, are shown. Neutrals (F radicals) density is supposed to be 10^{19} m^3. The simulation time is 100s, and it is divided in 100 equal etching intervals (Monte Carlo steps).

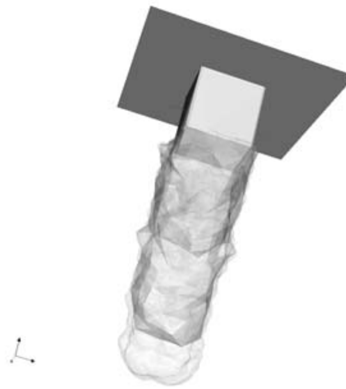

Fig. 4. Anisotropic etching - feature profiles at t = 0, t = 40 s, t = 80 s and t = 100 s.

These results show that realistic calculations requires much better statistic (greater number of particles) in the Monte Carlo step of the calculations, which is now limited by the available computational resources.

4. Electric field calculations

Finite difference method cannot be used when the geometry of the problem is irregular, as it is expected for the etching profiles. So, it is a natural choice to use finite elements method (although it is not the only possibility) for solving Poisson equation describing the electric field in the feature. This method requires remeshing before each flux calculation step. In three dimensions, it can be very difficult and time consuming. In this paper we shall present results of the electric field calculations for the profiles presented in Fig. 2, obtained for etching rates defined by $V = V_0 \cos\theta$.

The calculations of the electric fields in this paper are performed by integrating a general finite element solver GetDP [24] in our simulation framework. GetDP is a thorough implementation of discrete differential forms calculus, and uses mixed finite elements to discretize de Rham-type complexes in one, two and three dimensions. Poisson equation in its weak form is given by

$$\int_{\Omega} \varepsilon(\mathbf{r}) \nabla \phi(\mathbf{r}) \nabla w(\mathbf{r}) d\Omega = \int_{profile} \rho_s(\mathbf{r}) w(\mathbf{r}) dS \quad , \tag{13}$$

where $\phi(\mathbf{r})$ is the unknown electrostatic potential, $w(\mathbf{r})$ is an arbitrary test function, $\varepsilon(\mathbf{r})$ is dielectric permittivity function, and $\rho_s(\mathbf{r})$ profile surface charge density, obtained in the particle fluxes calculation step. The calculation domain Ω is a hexahedron, shown in Fig. 5c, divided by the profile surface in upper (air) and lower (non-etched material) parts.

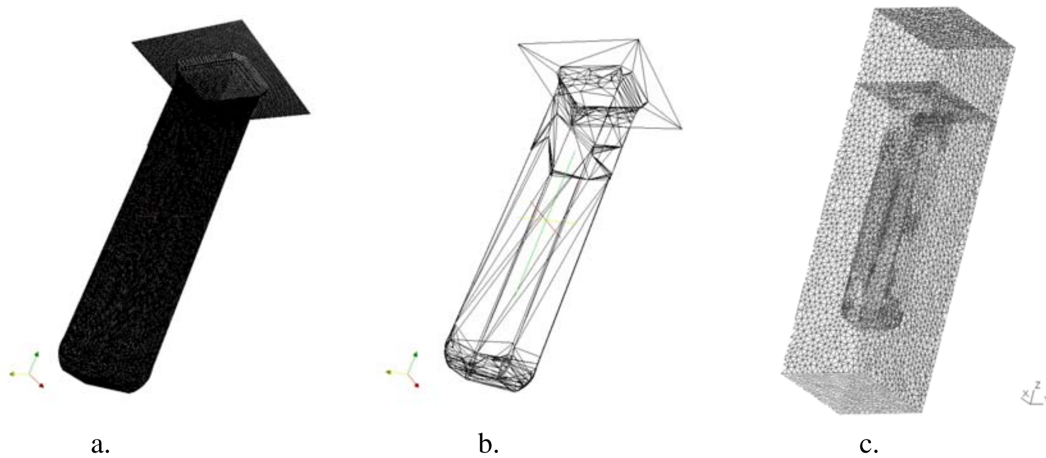

Fig. 5. Mesh generation steps: a) profile surface obtained from level set function (80216 triangles); b) simplified profile after quadric decimation (802 triangles); c) tetrahedral mesh (114786 tetrahedra)

In Fig. 5a the profile surface obtained from level set function (for t = 120s) using standard marching cubes algorithm is shown. It is made of more than 80000 triangles, and as such it is not convenient as an input for mesh generation program. This number should reduced first, by a proper surface simplification filter, while preserving important surface topology characteristics. In Fig. 5c the surface mesh of the tetrahedral mesh corresponding to the simplified profile is shown. On top and bottom surfaces zero Dirichlet conditions ($\phi(\mathbf{r}) = 0$) are imposed, while on vertical sides Neumann symmetry boundary conditions ($\mathbf{n}\nabla\phi(\mathbf{r}) = 0$) are applied.

Meshing of the computational domain is carried out by TetGen tetrahedral mesh generator [25]. TetGen generates the boundary constrained high quality (Delaunay) meshes, suitable for numerical simulation using finite element and finite volume methods. As a part of the post-processing procedure the electric fields, obtained on the unstructured meshes, are recalculated on the Cartesian rectangular domains containing the regions of the particles movement. In this manner, the electric field on the particles could be calculated by simple trilinear interpolation.

The calculations for the profile surfaces obtained for etching rates given by $V = V_0 \cos\theta$ show the electrostatic potential in the feature reaches a steady-state very quickly, comparing to the duration of the etching time step. These potential distributions in the feature and on the profiles are shown in Fig. 6. The maximal value of the potential at the bottom of the profile is smaller than the maximum ion energy, while the top surface is slightly negatively biased, as expected.

The time dynamic of the potential at the bottom is of special interest. The results showing this dependence are shown in Fig. 7. for the profiles from previous figure. The corresponding aspect ratios (height/width of the trench, AR) are marked on the figure.

The time necessary for the electric potential at the bottom of the feature to reach its steady-state value varies from ~1ms for smallest aspect ratio up to ~5ms for the highest. These numbers are considerably smaller then the values obtained in 2D simulations described in [18, 19], and especially then values obtained in 3D simulations published in reference [20]. Since these times are much shorter then etching time step Δt_{etch}, the organization of the whole simulation cycle can be significantly simplified.

Journal of Physics: Conference Series **86** (2007) 012017 doi:10.1088/1742-6596/86/1/012017

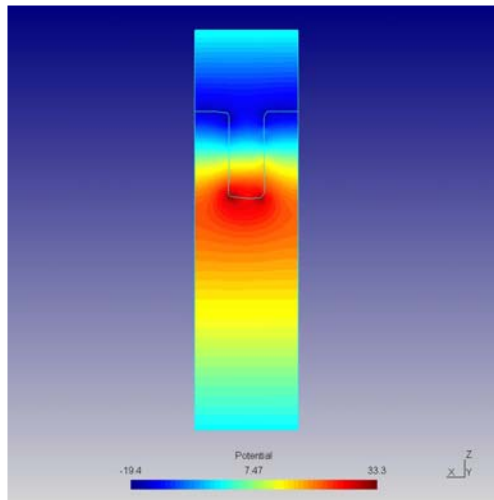

a.

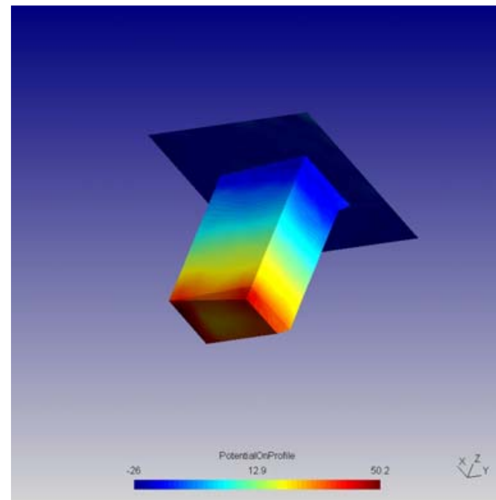

b.

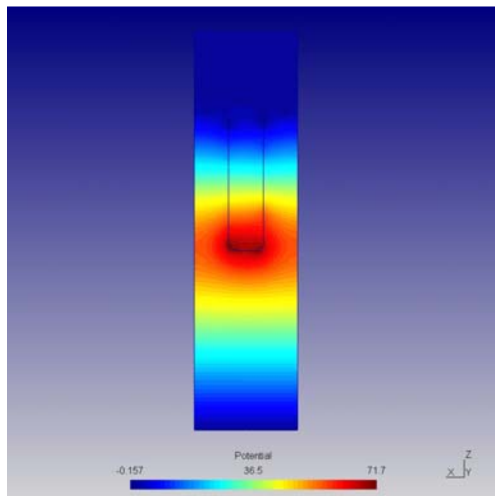

c.

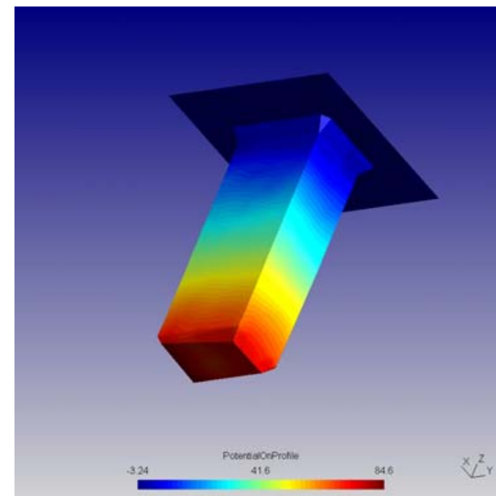

d.

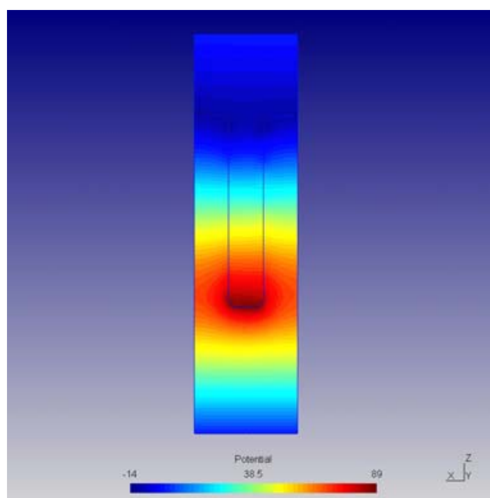

e.

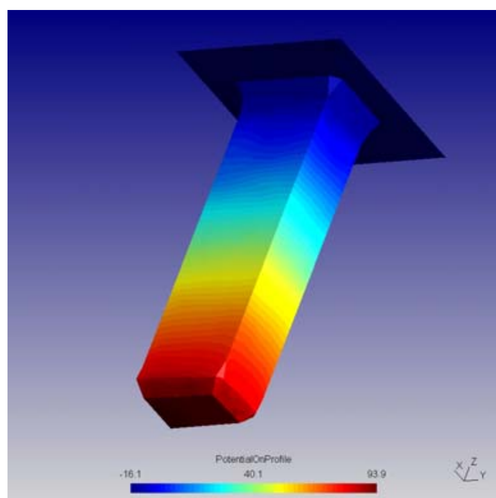

f.

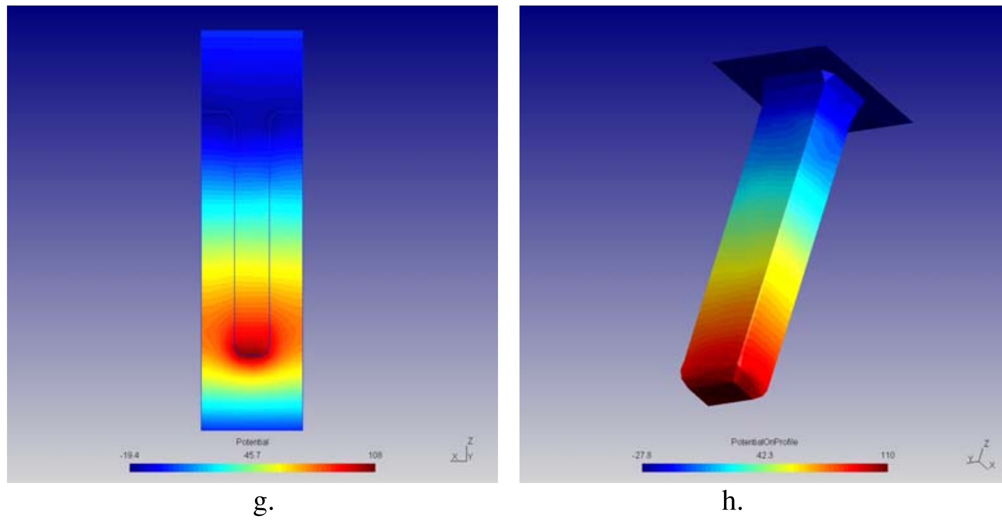

Fig. 6: Steady-state electrostatic potential in feature (on the left) and on the profile surface (on the right) for the profiles from Fig. 2: t = 30s (a, b), t = 60s (c, d), t = 90s (e, f) and t =120s (g, h)

In Fig. 8. the dependence of the bottom steady-state electrostatic potential on the aspect ratio is shown. This potential increases with the aspect ratio, which is in accordance with the results of [18].

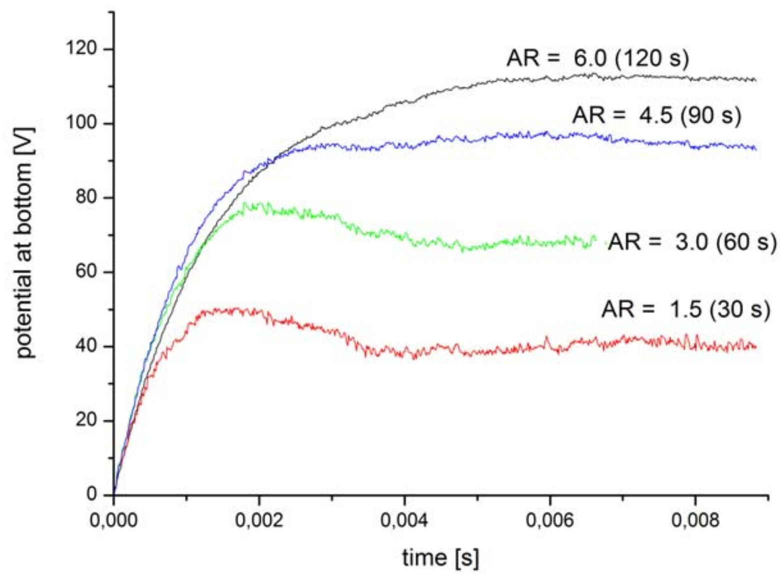

Fig. 7. Time dependence of the bottom potential for different aspect ratios (AR)

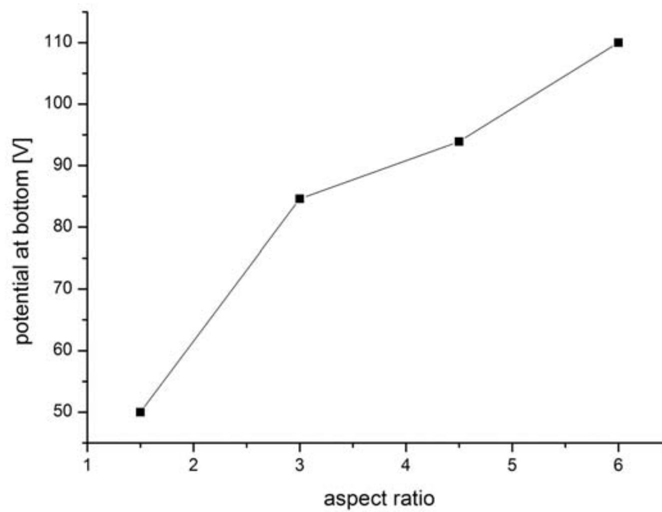

Fig. 8. Dependence of the bottom potential on the aspect ratio

5. Conclusion

Plasma processing is indeed one of the crucial modern technologies that have made a significant impact on fabrication of integrated circuits (IC) and consequently in electronics and consumer goods in general. Damage to ICs during manufacturing as a result of charging of the dielectrics during finalization of interconnects is both reducing the profitability and reducing the ability to reach large sizes of microchips and make complex system integration on a single chip. So, realistic three dimensional etching profile simulations are urgently needed, but still lacking.

Here we shall list some urgently needed improvements for our simulation framework. It is understandable that realistic calculations should include complex surface reactions set, the effects of the profile charging, polymer deposition, as well as better statistic (greater number of particles) in the Monte Carlo step of the calculations, which is now severely limited by the available computational resources. Realistic models of etching should be implemented in generic manner (contrary to the current *ad hoc* implementation), if possible, because it is not possible to know in advance what processes should be included in particular etching simulations. Monte Carlo module should be parallelized, and we are considering using GPU (graphics processing units) for that purpose [26], since it is probably the only possibility to obtain adequate computational performances on a desktop computer. GPU's has evolved into a highly parallelized multiprocessor machines over the last several years. Due to their increasing computational power and flexibility, they are becoming a very powerful computational platform for general-purpose computational problems. The latest results describing a Hamilton-Jacobi equation solver implemented on NVIDIA GeForce 8800 GTX GPU reports factor of 50-100 computational time reduction [27], comparing to Intel Core 2 Duo 2.4GHz CPU. Also, the 3D simulation of etching profile evolution requires a very robust mesh generation algorithm, together with a reliable update of geometry based on level set framework. Current mesh generation procedure based on Delaunay triangulation is not robust enough and other possibilities should be explored. Since we use level sets as the representation for etching profile, another method motivated by crystallography, is potentially very promising [28]. Mesh generation starts with a BCC (body-centered cubic) background mesh, that is adaptively refined with a red-green strategy, from which we carefully select a topologically-robust subset of tetrahedra that roughly match the level set etching profile. This candidate mesh is then “compressed” to match the level set boundary as closely as possible.

The results presented in this paper concerning the time necessary for the electric field in the feature to reach its steady-state value are potentially very important for the preparation of the whole

simulation cycle. Since the calculations show that this time is about several milliseconds, which is very short comparing to the etching time step Δt_{etch} (during which we assume that the etching rate is constant), it is reasonable to calculate steady-state values of the electric field in the beginning of every Monte-Carlo step and use this field subsequently, instead of devising a complex and time costly scheme for the recalculation of the field during particle fluxes calculations.

It is understandable that more realistic calculations should include the effects of polymer deposition, profile charging, more complex surface reactions set, as well as better statistic (greater number of particles) in the Monte Carlo step of the calculations, which is always limited by the available computational resources. We hope that an implementation of the Monte-Carlo module calculating particle fluxes on GPU, which is currently under development, will make realistic 3D simulations feasible.

Acknowledgements
The present work has been supported by the TESLA Project: Science with Accelerators and accelerator technologies (1247) and project 1478 financed by the Ministry of Science and Environmental Protection.

References
[1] Sethian J 1998 Level Set Methods and Fast arching Methods: Evolving Interfaces in Computational Geometry, Fluid Mechanics, Computer Vision and Materials Sciences (Cambridge University Press, Cambridge, UK)
[2] Osher S and Fedkiw R 2003 Level Set Method and Dynamic Implicit Surfaces (Springer-Verlag, New York, NY)
[3] Hoekstra R and Kushner M 1998 Journal of Vacuum Science and Technology A 16 (6) 3274
[4] Yoshida Y and Watanabe T 1983 Proceedings of the Symposium on Dry Processing pp. 4, (Tokyo)
[5] Hashimoto K 1994 Japanese Journal of Applied Physics 33 6013
[6] Hwang G and Giapis K 1997 Journal of Vacuum Science and Technology B15 (1) 70
[7] Whitaker R 1998 The International Journal of Computer Vision 29 203
[8] NLM Insight Segmentation and Registration Toolkit, http://www.itk.org
[9] Evans L 1998 Partial Differential Equations (American Mathematical Society, Providence) pp. RI
[10] Radjenović B, Lee J K and Radmilović-Radjenović M 2006 Computer Physics Communications 174 127
[11] Lieberman M and Lichtenberg A 1994 Principles of Plasma Discharges and Materials Processing (John Wiley & Sons, Inc.)
[12] Birdsall C K 1991 IEEE Transactions on Plasma Science 19 65
[13] Verboncoeur J P, Alves M V, Vahedi V and Birdsall C 1993 Journal of Computational Physics 104 321
[14] Radjenović B and Lee J K 2005 XXVIIth ICPIG (Eindhoven, the Netherlands 18-22 July, 2005)
[15] Mahorowala A and Sawin H 2002 Journal of Vacuum Science and Technology B 20 (3) 1084
[16] Yagisawa T, Maeshige K, Shimada T and Makabe T 2004 IEEE Trans. on Plasma Science 32 90
[17] Shimada T, Yagisawa T and Makabe T 2006 Japanese Journal of Applied Physics 45 8876
[18] Matsui J, Maeshige K and Makabe T 2000 Journal of Physics D: Applied Physics 34 2950
[19] Matsui J, Nakano N, Petrovic Z and Makabe T 2001 Applied Physics Letters 78 883
[20] Park H S, Kim S J, Wu Y Q and Lee J K 2003 IEEE Trans. on Plasma Science 31 703
[21] La Magna A and Garozzo G 2003 Journal of The Electrochemical Society 150 F178
[22] Zhang D, Rauf S, Sparks T and Ventzek P 2003 Journal of Vacuum Science and Technology B 21 (2) 828

[23] Hwang G S, Anderson C, Gordon M, Moore T, Minton T and Giapis K 1996 Physical Review Letters 77 3049
[24] GetDP: A General Environment for the Treatment of Discrete Problems (http://www.geuz.org/getdp)
[25] TetGen: A Quality Tetrahedral Mesh Generator and Three-Dimensional Delaunay Triangulator http://tetgen.berlios.de)
[26] Owens J, Luebke D, Govindaraju N, Harris M, Krüger H, Lefohn A and Purcell T 2007 Computer Graphics Forum 26 80
[27] Jeong W and Whitaker R 2007 University of Utah Technical Report UUCS-07-010
[28] Molino N, Bridson R, Teran J and Fedkiw R 2003 Proceedings of the 12th International Meshing Roundtable pp. 103